

THE PHYSICAL REVIEW

A journal of experimental and theoretical physics established by E. L. Nichols in 1893

SECOND SERIES, VOL. 135, NO. 5B

7 SEPTEMBER 1964

Solid State and Nuclear Results from Mössbauer Studies with $I^{129}\dagger$

D. W. HAFEMEISTER,* G. DEPASQUALI, AND H. DEWAARD‡

Department of Physics, University of Illinois, Urbana, Illinois

(Received 16 April 1964)

The Mössbauer effect of the 26.8-keV transition in I^{129} has been studied in a number of iodine compounds. The following results have been obtained: (a) The isomeric shifts for the alkali iodides were found to be linearly dependent on the number of $5p$ holes in the iodine ion. From this dependency, a calibration of the isomeric shift scale in terms of the $5s$ -electron density was obtained. The s and p populations inferred from these data are in sharp disagreement with those predicted by the simple theory of electronegativity. An explanation for this discrepancy is given. (b) From the calibration mentioned under (a), a relative change of nuclear radius $\Delta R/R = (R_{26.8} - R_{\text{gnd}})/R_{\text{gnd}} = 3 \times 10^{-5}$ is computed. (c) The isomeric shifts for some iodates indicate that their $5s$ -electron density is about 18% larger than that of the iodides. This increase is caused by the partial removal of $5p$ electrons from iodine in the I-O bonds, which results in reduced screening of the $5s$ electrons. The shift for potassium periodate implies that the $5s$ -electron density is decreased by 33% compared to the iodate. This decrease is attributed mainly to the sp hybridization of the I-O bonds in KIO_4 . The average charge removed per I-O bond, calculated from the isomeric shifts of the iodates and periodate, is $0.61 e$. (d) The quadrupole splitting of KIO_3 was used to determine the I^{129} quadrupole ratio, $Q_{26.8}/Q_{\text{gnd}} = 1.23 \pm 0.02$. The asymmetry of the iodate spectrum and the sign of the quadrupole moment show that the sign of the iodate field gradient is negative. The values of the quadrupole coupling constant, eqQ , at 80°K for KIO_3 and NH_4IO_3 are in agreement with nuclear-magnetic-resonance results and $eqQ_{127} = 1030 \pm 20$ Mc/sec for $Ba(IO_3)_2$. (e) The recoilless fraction f was found to deviate from 0.26 by less than 25% for all alkali iodides at 80°K .

I. INTRODUCTION

IN the past few years the Mössbauer effect¹ has been applied to a variety of problems in chemistry, nuclear physics, and solid-state physics. In this paper we discuss results obtained in these fields from Mössbauer experiments performed with the 26.8-keV, $\frac{5}{2}^+ \rightarrow \frac{7}{2}^+$ transition of I^{129} (Fig. 1). Preliminary results have already been reported.²

1. Chemical Physics

Because iodine has only one electron missing from a closed-shell configuration, it can form many different formal valence states. In Sec. III we discuss the three valence states of iodine that we have studied: 1^- in the

iodides, 5^+ in some iodates, and 7^+ in potassium periodate (KIO_4). The covalent bonding between the iodine and the oxygen atoms is an important feature of the latter two compounds. It should also be possible to study the 1^+ and 3^+ states of iodine which are unstable in inorganic compounds but do exist in organic compounds, e.g., iodoso- and iodoxybenzene.

The $5s$ -electron density at the iodine nucleus, which can be inferred from the isomeric shift measured for the compounds just mentioned, gives information about the nature of the chemical bond. The results on the isomeric shift in the iodides can be supplemented by data obtained from nuclear magnetic-resonance experiments (chemical shift and dynamic quadrupole resonance) which give information about the number of iodine $5p$ holes. In particular, the $5s$ -electron density at the nucleus depends rather sensitively on the relative participation of the $5p$ and $5s$ electrons in the bonds between iodine and the surrounding atoms.

A measurement of quadrupole splitting yields the field gradient at the nucleus if its electric quadrupole moment is known. Absolute values of the field gradients can in principle be obtained from quadrupole-resonance

† Supported in part by the U. S. Air Force Office of Scientific Research and by the Office of Naval Research.

* Submitted in partial fulfillment of the requirements for the degree of Doctor of Philosophy, University of Illinois. Present address: Los Alamos Scientific Laboratory.

‡ On leave of absence, University of Groningen, The Netherlands, 1962-63.

¹ Reviews of the Mössbauer effect can be found in: H. Frauenfelder, *The Mössbauer Effect* (W. A. Benjamin, Inc., New York, 1962), and A. Boyle and H. Hall, Rept. Progr. Phys. **25**, 441 (1962).

² H. deWaard, G. DePasquali, and D. Hafemeister, Phys. Letters **5**, 217 (1963).

measurements. In many cases, however, it is difficult to find such resonances, either because they are broadened and thus give a small effect or because they are very narrow and, therefore, hard to locate. Mössbauer experiments will give results in most cases, but they are generally less accurate. Yet, for cases where the spacing of the lines is larger than their width, an accuracy of the order of a few percent for the quadrupole-coupling constant is not hard to obtain. Such cases are represented by the iodates which are discussed in Sec. IV. Another feature of the Mössbauer effect is that the asymmetry of the hyperfine pattern which occurs when the spin of at least one of the nuclear states involved is larger than $\frac{3}{2}$ may be used to determine the sign of the field gradient.

2. Lattice Dynamics

The alkali halides are among the most studied compounds in solid-state physics. Their cubic structure and the ease with which large single crystals can be grown have made them attractive objects for lattice-dynamics studies. For instance, the elastic constants have been measured for most of the alkali halides and their phonon spectra are relatively well known from thermal neutron scattering. For a further understanding of the lattice dynamics of these crystals the recoilless fraction f is of interest. We have measured f at liquid-nitrogen temperature for LiI, NaI, RbI, and CsI, providing a wide range of alkali masses.

The recoilless fraction f is determined by an integration over the entire phonon spectrum. The Debye-model phonon spectrum has been used to compute f . Also some calculations of f for the NaCl lattice have been made by Kagan and Maslov.³ In Sec. VI we compare the results of our measurements with these calculations. It should be possible in principle to calculate f for the alkali iodides directly from their experimentally determined phonon spectra.

3. Nuclear Physics

On first sight it would seem that the fact that iodine has only three protons outside the closed shell $Z=50$ should facilitate the calculation of its nuclear properties. However, our values of the electric quadrupole moment, the change of nuclear radius, and the lifetime of the 26.8-keV state all show that no simple explanation on the basis of the shell model is possible. The nuclear results are discussed in Sec. V.

4. Experimental Problems

Mössbauer absorptions of 10% or more can be readily obtained with I^{129} . Linewidths for thin absorbers are not too much larger than the width estimated from the lifetime of the level. In carrying out an I^{129} Möss-

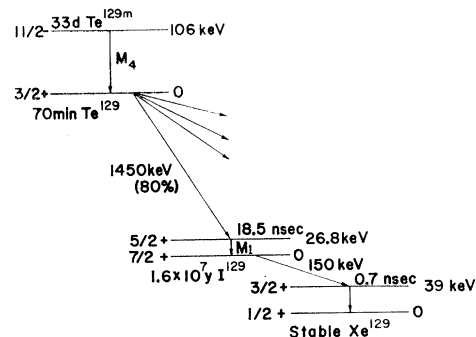


FIG. 1. The Te^{129m} - I^{129} - Xe^{129} decay scheme.

bauer experiment, however, the following experimental restrictions must be considered:

(1) The decay of the ground state of I^{129} (1.6×10^7 yr) imposes some conditions on the preparation of absorbers. Proper care must be taken to contain the radioactive iodine. It is desirable to use high-yield procedures in preparing the absorber materials. Radiations from the I^{129} decay need not dilute the effect appreciably because they can largely be removed by a critical absorber (Sec. II.1).

(2) In order to avoid the 27.2-keV x rays resulting from the 106-keV, 33-day excited state of Te^{129} , we have used the short lived 70-min ground state of Te^{129} . Because of the short lifetime, it is necessary to perform the experiment within a reasonable distance from a reactor.

(3) The high spins ($\frac{5}{2}^+$ and $\frac{7}{2}^+$) of the nuclear states involved cause the hyperfine spectra to consist of many components (8 for quadrupole splitting and 18 for magnetic splitting). Therefore, large electric-field gradients and large magnetic fields are needed to resolve the hyperfine structure of the spectra.

(4) Since most iodine compounds are not tightly bound ($\theta \sim 120^\circ K$), the absorbers must be at least cooled to liquid-nitrogen temperature.

II. EXPERIMENTAL PROCEDURE

1. General Remarks

The Mössbauer effect in I^{129} was first observed by Jha, Segnan, and Lang⁴ who used the 33-day, 106-keV isomeric state of Te^{129} as the source (see Fig. 1). We have made the following two major changes: (1) In order to avoid the 27.2-keV x rays from the internal conversion of the 106-keV state in Te^{129} , we have used the 70-min ground-state activity of Te^{129} . This state predominately decays to the 26.8-keV level of I^{129} and is produced by irradiating Te^{128} in a reactor. Since the cross section for the production of Te^{129} in the ground state is much larger than that of the 106-keV isomeric state and because the ground-state half-life is very much

³ Yu. Kagan and V. A. Maslov, Zh. Eksperim. i Teor. Fiz. 41, 1296 (1961) [English transl.: Soviet Phys.—JETP 14, 922 (1962)].

⁴ S. Jha, R. Segnan, and G. Lang, Phys. Rev. 128, 1160 (1962).

shorter, almost all activity comes from the ground state.⁵ (2) The I^{129} in the absorber decays by β emission ($E_0=150$ keV, $T_{1/2}=1.6\times 10^7$ yr) to the 40-keV excited state of Xe^{129} . The 40-keV Xe γ rays⁶ are strongly converted giving an x ray of 29.4 keV. Since this x ray and the 26.8-keV γ ray cannot be resolved by a scintillation counter, we have inserted a 70-mg/cm² selectively absorbing In foil between the I^{129} absorber and the scintillation detector. This foil reduces the number of xenon x rays by a factor of 11 and the 26.8-keV γ rays by a factor of 2. The position and thickness of the foil are critical since the 24.0-keV x rays of the In also contribute to the background. We have optimized both position and thickness so as to maximize the signal to background ratio.

2. Apparatus

Source and absorber were cooled to liquid-nitrogen temperature in a simple cryostat constructed out of styrofoam and copper (Fig. 2). The absorber is rigidly fixed to an aluminum cooling plate and the copper source holder is fastened by two flexible corrugated copper foils to a second aluminum plate. These plates extend into the nitrogen bath and are rigidly clamped together and to the styrofoam. A fixed nitrogen level was maintained in order to keep the source and absorber temperature between 78 and 80°K.

Because of the short half-life of Te^{129} , it was necessary to use a velocity sweep system rather than a constant velocity drive. The sinusoidal motion of a twin loud-speaker system mounted outside the cryostat is transferred to the source by a Lucite rod entering the cryostat through two rubber membranes. In this way moisture is kept from entering the cryostat while the air insulation between the foils prevents the formation of ice on the outer foil. One loudspeaker was driven by a type-200 CD Hewlett Packard audio oscillator with a transformer for impedance matching. Frequencies between 20 and 40 cps have been used, generally close to the mechanical resonance frequency of 30 cps. The sine wave from the pick-up coil is amplified in a low-drift amplifier and fed into the base line input of a 400-channel RIDL analyzer. Pulses from the 26.8-keV line are routed to one group of 200 channels, while pulses from a part of the spectrum that does not exhibit resonance absorption are routed to the other group of 200 channels. The spectra were normalized by dividing the counts in the

⁵ As the source decays, the signal to background ratio decreases. For this reason there exists an optimum measuring time t for which the statistical accuracy of the information reaches a maximum that can be derived from

$$2(N_a/N_s)(t/\tau) = (e^{-t/\tau} - 1)[1 - (N_a e^{t/\tau}/N_s)],$$

where N_s is the initial activity of the source, N_a the background activity from the absorber, and τ the mean life of the source. For a typical case ($N_s=400\ 000$ counts/min, $N_a=40\ 000$ counts/min), $t_{opt}=2.75\tau=275$ min. Because the maximum is quite flat, this optimum time need not be observed very strictly.

⁶ These γ rays are utilized in the Xe^{129} Mössbauer experiments of G. J. Perlow and M. R. Perlow, Rev. Mod. Phys. 36, 353 (1964).

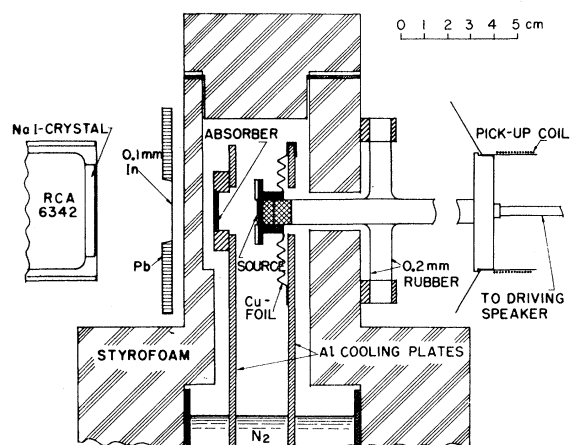


FIG. 2. Experimental arrangement.

first group of channels by those in the second group. Before and after each iodine run, the velocity scale of the spectrometer was calibrated to an accuracy of about 1% with the well known Mössbauer spectrum of a source of Co^{57} in iron and an enriched Fe^{57} absorber.

3. Sources and Absorbers

Sources of $Zn^{66}Te^{128}$ (cubic), $PbTe^{128}$ (cubic), and $Cr_xTe_y^{128}$ (ferromagnetic) were used. The ground state of Te^{129} was produced by irradiating the Te^{128} compounds for 90 min in a flux of 7×10^{11} thermal neutrons/cm²-sec in the University of Illinois reactor. With our geometry we obtained an average of approximately 10^5 counts per channel over 200 channels for each 3-h run. Separated Zn^{66} (98.8% enriched) and Te^{128} (94.4% enriched) isotopes were used for preparing the $ZnTe$ in order to reduce activities from the other Zn and Te isotopes. Because the neutron activation of Cr and Pb is relatively small, it was not necessary to use their separated isotopes. Radiation damage to the source was unimportant as annealing the $Zn^{66}Te^{128}$ after irradiation did not change the intensity or width of the lines. Since a source which was irradiated 50 times gave reproducible results, long term radiation damage was also negligible.

The sources were formed at 1100°C in an evacuated quartz tube. The $ZnTe$ samples were annealed at 800°C for one hour to remove internal strains. The compounds were powdered and sedimented from toluene containing polystyrene cement (Q dope) onto a 0.005-in. Mylar foil. A 0.001-in. Mylar foil was cemented over the dried compound.

The I^{129} compounds, some of them highly deliquescent, were placed in double O-ring sealed containers. The absolute thicknesses of the I^{129} absorbers were determined to an accuracy of about 6% by measuring their activity, correcting for self-absorption and then comparing to the counting rate of a single crystal of $Ba(I^{129}O_3)_2$ for which the mass was known. The relative

thicknesses were determined with a higher accuracy than the absolute thickness. The alkali iodide powders were mixed in a dry box with dry silica gel (SiO_2) powder in order to get a more uniform distribution of I^{129} especially for very thin absorbers.

The iodine (86% I^{129}) was purchased from Oak Ridge in a basic solution of NaOH and NaI. The high yield processes (>95%) employed to make the absorbers are discussed in Ref. 2.

III. THE ISOMERIC SHIFT

1. Theoretical Considerations

The isomeric shift δ is the energy difference of the emitted and absorbed γ -ray transitions resulting from the difference of the s -electron densities in source and absorber.⁷ For Mössbauer experiments, δ is usually expressed as the Doppler velocity needed to compensate for this energy difference and we will call δ positive when source and absorber move towards each other.⁸ Thus a positive δ corresponds to an absorber transition energy higher than that of the source.

An expression for δ in terms of the source and absorber s -electron densities at the origin, $|\Psi_s(0)|^2$ and $|\Psi_a(0)|^2$, respectively, can be obtained by considering the electrostatic interaction between the s electrons and

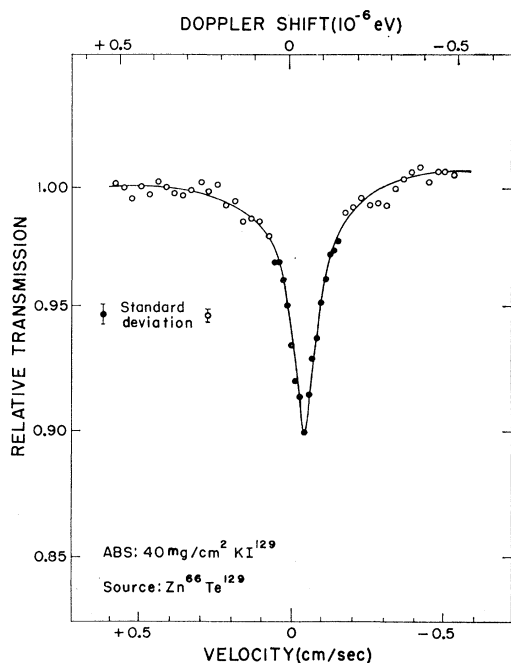


FIG. 3. Relative transmission of 26.8-keV γ rays from a $\text{Zn}^{66}\text{Te}^{129}$ source through a KI^{129} absorber as a function of source velocity.

⁷ By using the alkali iodide Debye temperatures of Table III, we have shown that the additional shifts due to the second-order Doppler shift at 80°K can be neglected.

⁸ The δ sign convention is opposite to the one used in our previous communication; it now agrees with the majority of the other authors.

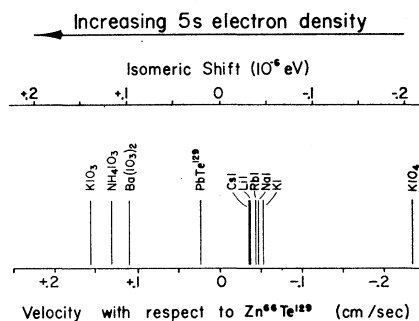


FIG. 4. Isomeric shifts in the I^{129} compounds. A positive velocity corresponds to the ZnTe source moving towards the absorber.

a nucleus with a uniform charge density. A relativistic calculation yields⁹

$$\delta = \frac{c}{E_\gamma} \frac{2\pi a_0^{2-2\rho} 2^{2\rho} e^2 (1+\rho)}{Z^{1-2\rho} [\Gamma(2\rho+1)]^2 2\rho(2\rho+3)(2\rho+1)} \times [R_{\text{ex}}^{2\rho} - R_{\text{gnd}}^{2\rho}] [|\Psi_a(0)|^2 - |\Psi_s(0)|^2], \quad (1)$$

where E_γ is the γ -ray energy, a_0 the Bohr radius, $\rho = (1 - \alpha^2 Z^2)^{1/2}$, and R_{ex} and R_{gnd} the nuclear radii for the excited state and the ground state, respectively. For the case of I^{129} ($Z=53$, $A=129$, $R=1.2 \times 10^{-13} A^{1/3}$ cm = 6.06×10^{-13} cm) Eq. (1) becomes

$$\delta = 2.23 \times 10^{-23} (\Delta R/R) \times [|\Psi_a(0)|^2 - |\Psi_s(0)|^2] \text{ cm/sec}, \quad (2)$$

where $\Delta R/R = (R_{\text{ex}} - R_{\text{gnd}})/R_{\text{gnd}}$. We will show in Sec. III.2 that a positive δ corresponds to an s -electron density greater than that of the ZnTe source.

In order to be able to use Eq. (2) for the determination of s -electron density differences, it must be "calibrated," i.e., source-absorber or absorber-absorber combinations must be found for which the s -electron density difference is known. (It is impossible to calculate the difference of the 2ρ th powers of excited and ground-state charge radii with any confidence from presently available nuclear models.) The most common method for calibrating the isomeric shift formula is to measure isomeric shifts for absorbers with different numbers of outer-shell s electrons, e.g., by using compounds with the absorbing atoms in different valence states. The accuracy of this method depends on how much is known about the chemical bonds in suitably chosen absorber compounds, in particular about their ionicity and their hybridization. $|\Psi(0)|^2$ can be obtained from Hartree-Fock calculations or it can be found for an outer s electron from the Fermi-Dirac formula¹⁰:

$$|\Psi(0)|^2 = \frac{1}{\pi a_0^2} \frac{Z Z_{\text{eff}}^2}{n_a^3} (1 - d\sigma/dn), \quad (3)$$

⁹ G. Breit, Rev. Mod. Phys. **30**, 507 (1958).

¹⁰ H. Kopfermann, Nuclear Moments (Academic Press Inc., New York, 1958), p. 144.

TABLE I. The alkali iodide, ZnTe, and PbTe isomeric shifts; number of iodine-ion p holes calculated by Menes and Bolef from chemical shift data and dynamic quadrupole resonance data; the alkali iodine electronegativity difference; the fractional deviation of the iodine-ion $5s$ -electron density from the $5s^25p^6$ closed-shell iodine-ion density computed from the isomeric shift data, Eq. (8), and $\delta_0 = -0.055$ cm/sec; the alkali ion polarizability; and the type of lattice.

Compound	Isomeric shift cm/sec wrt ZnTe + = towards	Number of p holes (h_p)		Electro- negativity difference ^c	$\Delta \Psi_{5s}(0) ^2/ \Psi_0(0) ^2$	Alkali ion polariza- bility ^d	Lattice ^e
		from chem. shift ^a	from dynamic quad. ^b				
LiI	-0.038 ± 0.0025	0.112		1.5-1.55	+0.014	0.029	NaCl
NaI	-0.046 ± 0.0025	0.040	0.085	1.6	+0.0075	0.408	NaCl
KI	-0.051 ± 0.0025	0.033	0.035	1.7	+0.0034	1.334	NaCl
RbI	-0.043 ± 0.0025	0.055	0.070	1.7	+0.010	1.979	NaCl
CsI	-0.037 ± 0.0025	0.165	0.165	1.75-1.8	+0.015	3.335	CsCl
ZnTe	0			0.9-1.0	+0.046		Zinc blende
PbTe	$+0.022 \pm 0.005$			0.7-0.9	+0.065		NaCl

^a See Ref. 11.

^b See Ref. 12.

^c See Ref. 20.

^d See Ref. 16.

^e See Ref. 24.

where Z_{eff} is the effective charge seen by the outer s electron, n_a is the effective quantum number, and $d\sigma/dn$ is the derivative of the quantum defect with respect to the n th quantum state. The former procedure has been used for Fe⁵⁷ while the latter has been used for Sn¹¹⁹, Au¹⁹⁷, and Eu¹⁵¹.

In iodine compounds other than the alkali iodides, the nature of the chemical bonds is not known sufficiently well to determine the s -electron density directly and therefore other means must be used. We have been able to combine the isomeric shift data in the alkali iodide series with the corresponding NMR chemical shift data to obtain the calibration (Sec. III.2) In Sec. III.3 a qualitative explanation of the isomeric and chemical shift data in the alkali iodides is discussed and in III.4 the iodate and periodate results are presented and interpreted.

2. Calibration of the I¹²⁹ Isomeric Shift Scale with the Isomeric and NMR Chemical-Shift Data

The alkali iodide isomeric shifts relative to ZnTe (Fig. 3) are displayed in Table I and in Figs. 4 and 5. The shift for a compound was determined by taking the center of gravity of the absorption line of each run and then averaging over all the runs. The errors assigned to the isomeric shifts were determined from the consistencies of the individual runs (Fig. 5) and from the uncertainties in the calibration of the spectrometer.

Data on the number of iodine $5p$ electrons are available from the NMR chemical shift measurements of Bloembergen and Sorokin¹¹ and from the dynamic quadrupole-coupling measurements of Menes and Bolef.¹² In the first method, the change of the magnetic field at the nucleus caused by the paramagnetism of the $5p$ electrons is measured. In the second, the attenuation of a sound wave caused by the nuclear spin-phonon interaction is measured. Both of these effects are proportional to the number of $5p$ holes, $h_p = 6 - y$, where the I⁻ configuration may be written

as $5s^25p^y$. The xenon configuration corresponds to $h_p = 0$ and $y = 6$. The values of h_p determined by these workers are compared to the isomeric shifts of the alkali iodides in Fig. 5 and Table I. The behavior of h_p is similar to that of the isomeric shift, and we can assume from this that the I⁻ $5s$ -electron density as measured by the Mössbauer effect is linearly dependent on the number of $5p$ holes, h_p . This linearity is not surprising since the changes of electron populations, $\Delta h_p \sim 0.1$, in the alkali iodides are quite small.

The linear dependence between δ and h_p can be used to calibrate the I¹²⁹ isomeric shift scale in the following fashion: An increase in the number of $5p$ electrons will decrease $|\Psi(0)|^2$ by increasing the shielding of the $5s$ electrons (Z_{eff} will be decreased for the $5s$). This effect may be expressed quantitatively by using Slater's shielding coefficients¹³ and the Fermi-Segrè formula, Eq. (3). If the numbers of electrons, N_i , in the various

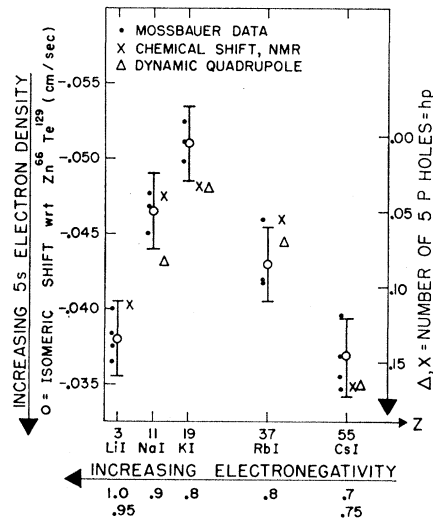


Fig. 5. The isomeric shifts (δ) and the number of iodine p holes, h_p , [X (Ref. 11), Δ (Ref. 12)] versus alkali atomic number for the alkali iodides. The data points for each alkali are spread horizontally for the sake of clarity.

¹¹ N. Bloembergen and P. Sorokin, Phys. Rev. **110**, 865 (1958).

¹² M. Menes and D. Bolef, Phys. Chem. Solids **19**, 79 (1961).

¹³ J. Slater, Phys. Rev. **36**, 57 (1930).

TABLE II. Iodide, iodate, and periodate isomeric shifts and corresponding 5s-electron densities computed from Eq. (8) and $\delta_0 = -0.055$ cm/sec.

Compound	Isomeric shift cm/sec wrt ZnTe + = towards	$\Delta \Psi_{5s}(0) ^2/ \Psi_0(0) ^2$
KI	-0.051 ± 0.0025	+0.0034
KIO ₃	$+0.156 \pm 0.02$	+0.18
NH ₄ IO ₃	$+0.131 \pm 0.020$	+0.16
Ba(IO ₃) ₂	$+0.111 \pm 0.02$	+0.14
KIO ₄	-0.234 ± 0.006	-0.15

shells are known, Slater's empirical shielding coefficients D_i can be used to obtain Z_{eff} by the relation

$$Z_{\text{eff}} = Z - \sum_i D_i N_i; \quad (4)$$

for I⁻ this becomes ($D_1 = D_2 = D_3 = 1$, $D_4 = 0.85$, $D_5 = 0.35$, $N_1 = 2$, $N_2 = 8$, $N_3 = N_4 = 18$, and $N_5 = 7 - h_p$)¹⁴

$$Z_{\text{eff}}(\text{I}^-) = 7.25 + 0.35h_p. \quad (5)$$

The relative change in the 5s-electron density can now be obtained from this equation and from the Fermi-Segrè formula where $|\Psi(0)|^2 \propto Z_{\text{eff}}^2$. We obtain for $h_p \ll Z_{\text{eff}}$

$$\Delta Z_{\text{eff}}^2 / Z_{\text{eff}}^2 = \Delta |\Psi_{5s}(0)|^2 / |\Psi_0(0)|^2 = 0.097(h_p^{(1)} - h_p^{(2)}), \quad (6)$$

where $h_p^{(1)}$ and $h_p^{(2)}$ are the numbers of 5p holes for alkali iodides (1) and (2) and $|\Psi_0(0)|^2$ is the 5s-electron density at the nucleus for the completely filled s and p shells. Equation (6) demonstrates the linear increase of 5s density as the number of p holes is increased. It is interesting to note that one 5p hole ($h_p = 1$) increases the 5s density by 10% which is in accordance with the results of the isotope shift.¹⁰ On the other hand, the change in isomeric shift for two different alkali iodides can be written according to Eq. (2) as

$$\Delta\delta = \delta^{(1)} - \delta^{(2)} = \text{const} \Delta |\Psi_{5s}(0)|^2 / |\Psi_0(0)|^2. \quad (7)$$

The best value of the calibration constant in this equation has been found by a least-squares fit between the δ and h_p data (Table I and Fig. 5). Combining Eqs. (6) and (7), we obtain

$$\Delta |\Psi_{5s}(0)|^2 / |\Psi_0(0)|^2 = 0.84\Delta\delta \quad (\delta \text{ in cm/sec}). \quad (8)$$

This value of the calibration constant cannot be regarded as very accurate (about 25%) because of certain approximations made in the work of Menes and Bolef and of Bloembergen and Sorokin and the approximate nature of Eq. (6). It should also be remarked that the chemical shift corresponding to the closed electron shell is not very accurately known.¹⁵ This uncertainty, however, does not affect the calibration constant in Eq. (8). The least-squares fit also gives

¹⁴ The 5s electron for which Z_{eff} is calculated is not counted.

¹⁵ R. Baron, J. Chem. Phys. **38**, 173 (1963).

the shift for the closed shell ($h_p = 0$) relative to ZnTe, $\delta_0 = -0.055$ cm/sec. The values of $\Delta |\Psi_{5s}(0)|^2 / |\Psi_0(0)|^2$ in Tables I and II are calculated from Eq. (8) relative to δ_0 .

The combination of Eqs. (2) and (8) shows that the sign of $\Delta R/R$ is positive. Its magnitude is computed in Sec. V.2.

3. Interpretation of the Alkali Iodide Data

The alkali iodide data of Sec. III.2 show that the idealized model of ionic crystals is inadequate since $\delta \neq \text{constant}$ and $h_p \neq 0$. An interpretation of the data must consider the effects on the iodine 5p population by covalency, deformation of the charge cloud by electrostatic interaction, and deformation by overlap. These three phenomena have a much smaller direct effect on the s electrons than on the p electrons. In this section we shall first discuss covalency and then the electrostatic interaction. In order to determine the effect of overlap, it is necessary to use the Hartree-Fock wave functions. Our attempt to use the phenomenological Born-Mayer theory¹⁵ for the overlap has been unsuccessful.

From the simple theory of electronegativity an approximately linear relation between the isomeric shift and the alkali electronegativity is expected, as will be shown below. This trend is seen when going from LiI to KI (Fig. 5), but is not observed for RbI and CsI. It is not surprising that effects other than electronegativity should appear in the alkali iodide δ data since the alkali electronegativity changes by only 20% while the alkali ionic radius changes by a factor of 2 and the polarizability¹⁶ changes by a factor of 110.

The electronegativity concept has been used in the past^{17,18} in discussions of s-electron density because it accounted reasonably well for the observed δ 's. Electronegativity χ is a measure of the electron seeking power of an atom, and is empirically defined as^{19,20}

$$\chi = 0.18(i + e), \quad (9)$$

where i is the ionization energy of the atom and e is its electron affinity, both measured in electron volts. The electronegativity of iodine²⁰ is 2.5 and the alkali electronegativities are indicated in Fig. 5 and in Table I. All proposed formulas²¹ indicate an increased ionicity I , the ionic fraction of the bond, with an increased elec-

¹⁶ J. R. Tessman, A. H. Kahn and W. Shockley, Phys. Rev. **92**, 890 (1953).

¹⁷ A. Aleksandrov, N. Delyagin, K. Mitrofanov, L. Polak, and V. Shpinel, Zh. Eksperim. i Teor. Fiz. **43**, 1242 (1963) [English transl.: Soviet Phys.—JETP **16**, 879 (1963)].

¹⁸ A review of the isomeric shift and the $\Delta R/R$ values for various nuclei is given by D. A. Shirley, Rev. Mod. Phys. **36**, 339 (1964). His calculated value of $|\Psi_0(0)|^2$ is considerably smaller than ours with the result that $\Delta R/R$ would be much bigger. He intended to make the sign of $\Delta R/R$ for I²⁰⁹ positive.

¹⁹ T. P. Das and E. L. Hahn, Nuclear Quadrupole Resonance Spectroscopy (Academic Press Inc., New York, 1958), p. 141.

²⁰ W. Gordy and W. Thomas, J. Chem. Phys. **24**, 439 (1956).

²¹ Y. P. Varshni and R. C. Shukla, Rev. Mod. Phys. **35**, 130 (1963).

tronegativity difference, $\Delta x = |x_1 - x_2|$, between the two members of the bond. For small changes of the alkali electronegativity, this can be expressed as

$$I = A + B\Delta x, \quad (10)$$

where A and B are empirical constants. For a completely ionic bond I must be 1, for a completely covalent bond, $I=0$. For the alkali iodides the ionicity and hence the number of iodine $5p$ electrons, $y=5+I$, should increase from LiI to CsI since the electronegativity difference between iodine and the alkali increases. This implies that for CsI the iodine ion configuration, $5s^25p^y$, should most closely approach the $5s^25p^6$ xenon configuration. Since $|\Psi(0)|^2$ is decreased by an increase in $5p$ population, we would expect on the basis of electronegativity alone that $|\Psi(0)|^2$ would decrease monotonically from LiI to CsI since their bonds have become more ionic.

These electron transfer trends can be expressed quantitatively by using Eq. (6) with the ionicity concept, Eq. (10). Since $I=1-h_p$, we obtain for $Cx_{\text{alk}} \ll 1$

$$|\Psi_{5s}(0)|^2 \propto (1 + Cx_{\text{alk}}). \quad (11)$$

The value of C can be determined from the empirical constants A and B of Eq. (10). The most accepted values of A and B were obtained by Gordy²⁰ and Dailey and Townes.²² We find $C=0.048$ for those of Gordy. Using the isomeric shift scale calibration, Eq. (8), we find $C=0.05$ for the linear part of our isomer shift curve (LiI to KI in Fig. 5). These values are in reasonable agreement. However, since RbI and CsI deviate completely with Eq. (11), we must investigate the effects of the electrostatic interaction and overlap.

It may be remarked here that a serious deviation from the electronegativity expectations has so far not been found for other Mössbauer nuclei. In particular, Aleksandrov *et al.*¹⁷ and others¹⁸ have found a linear relation between δ and Δx for the tin tetrahalides. This result is not surprising since Δx is much larger for the halogens than for the alkalis, and therefore the difference in ionicity is much more important for the tin tetrahalides than for the alkali iodides.

The simple theory of electronegativity fails in this discussion because it is based merely on electron-transfer energies [Eq. (9)] and determines only the approximate number of electrons transferred. The experimental results can at least be qualitatively explained by taking into account the deformation of the ground state wave functions by the electrostatic interaction between the cation-anion electron clouds. As suggested by Flygare, the perturbed iodine $5p'$ wave function can be expressed to first order by

$$\Psi_{I-5p'} = (1-b^2)^{1/2}\Psi_{I-5p} + \sum_L \sum_N b_{LN}\Psi_{I-N}, \quad (12)$$

where

$$b^2 = \sum_L \sum_N b_{LN}^2 = \sum_L \sum_N \frac{\langle \Psi_{M+L}\Psi_{I-N} | \sum_{ij} (e_i e_j / r_{ij}) | \Psi_{I-5p}\Psi_{M+0} \rangle}{E_{M+0} - E_{M+L} + E_{I-5p} - E_{I-N}},$$

²² B. P. Dailey and C. H. Townes, *J. Chem. Phys.* **23**, 118 (1955).

b^2 is the fraction of the iodine $5p$ ground state which is excited to higher states, Ψ_{I-5p} and Ψ_{I-N} (E_{I-5p} and E_{I-N}) are the iodine $5p$ ground-state and excited-state wave functions (energies), Ψ_{M+0} and Ψ_{M+L} (E_{M+0} and E_{M+L}) are the alkali ground-state and excited-state wave functions (energies), and r_{ij} is the distance from the i th iodine charge to the j th alkali charge. Equation (12) neglects the deformation due to overlap.

Since the dipole-dipole term is the predominant term in the multipole expansion of the electrostatic interaction, b^2 can be approximated²³ by

$$b^2 = 3\alpha_{M+}\alpha_{I-}E_M E_I / 2r^6(E_M + E_I)^6, \quad (13)$$

where α_{M+} and α_{I-} are the alkali-ion and iodine-ion polarizabilities, E_M and E_I are the average excitation energies of the alkali and iodine, and r is the alkali-iodine separation distance. Because the alkali polarizability¹⁶ increases by a factor of 110 from Li to Cs (Table I), the fraction b^2 of the $5p$ electron excited to higher states will increase from LiI to CsI. Thus the multipole interaction decreases the $5p$ population from LiI to CsI whereas electronegativity increases it. This interaction causes the iodine ion in the more polarizable Rb and Cs iodides to have a smaller $5p$ population and consequently a larger $|\Psi(0)|^2$ than expected from the electronegativity arguments [Eq. (11)].

4. Isomeric Shifts in Some Iodates and in Potassium Periodate

In Table II, the isomeric shifts relative to the ZnTe source and the relative change of $|\Psi(0)|^2$ (see Sec. III.2) are given for KI, KIO₃, NH₄IO₃, Ba(IO₃)₂, and KIO₄ absorbers. From this table as well as from Fig. 4, in which all the isomeric shift data have been collected, it is clear that I⁻, (IO₃)⁻, and (IO₄)⁻ shifts fall into three distinct groups. The (IO₃)⁻ and (IO₄)⁻ shifts relative to I⁻ may be qualitatively explained as follows: In the alkali iodides, the I⁻ ion almost has the xenon configuration $5s^25p^6$. X-ray diffraction data^{24,25} show that in (IO₃)⁻ compounds each I atom is surrounded by six O atoms in an irregular octahedron with three of the O's in the (IO₃)⁻ group and the other three at a considerably greater distance. Since the resulting I-O bond angles are very close to 90°, the bonds will contain chiefly $5p$ electrons (small sp hybridization¹⁹). Removal of $5p$ electrons from atomic orbits increases $|\Psi(0)|^2$, and raises the energy of the γ transition. In the (IO₄)⁻ ion, each iodine atom is surrounded by a tetrahedron of oxygen atoms with 109° angles between the I-O bonds.²⁴ There should now be a considerable sp hybridization leading to a removal of $5s$ electrons from the atomic orbits of iodine. The decrease of $|\Psi(0)|^2$ shifts the γ line to a lower energy, below that of I⁻.

²³ H. Margenau, *Rev. Mod. Phys.* **11**, 1 (1939).

²⁴ R. Wyckoff, *Crystal Structures* (Interscience Publishers, Inc., New York, 1960).

²⁵ C. H. MacGillavry and C. L. P. van Eck, *Rec. Trav. Chim.* **62**, 729 (1943).

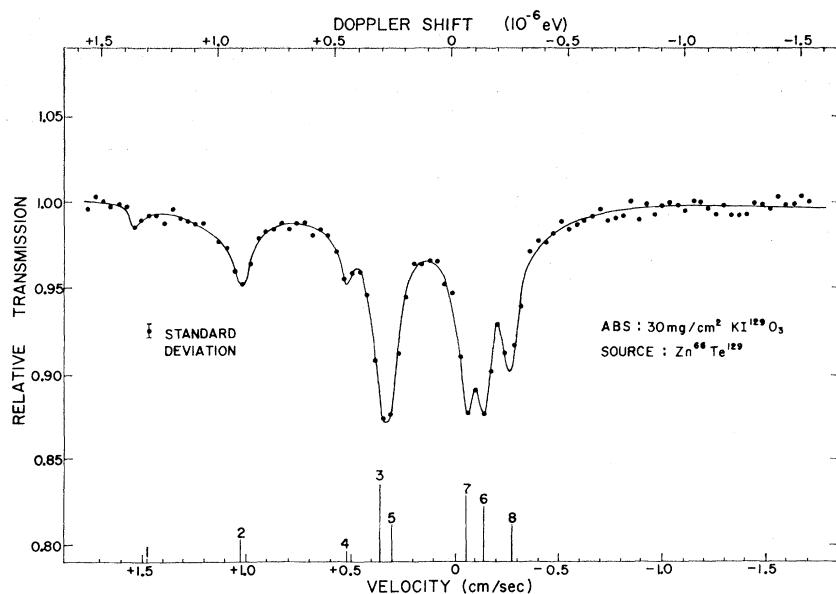


Fig. 6. Relative transmission through KIO_3 . The vertical lines represent the calculated positions and relative intensities resulting from the quadrupole interaction.

Thus, there are two counteracting effects of $|\Psi(0)|^2$; an increase caused by the removal of $5p$ electrons, and a decrease caused by the removal of s electrons in hybridized sp bonds.

In the following we will attempt to derive some more quantitative results from our δ data. The sizable quadrupole coupling of the iodates, combined with the x-ray data just quoted,²⁵ indicate that the iodine bonds to three of the surrounding O atoms are much stronger than those to the other three. Hence, the six I-O bonds remove different amounts of charge from the iodine atom. Assuming the charge on the O atoms to be the same in the iodates and the periodates, we find the charge ΔZ removed from the $n=5$ closed shell of an I- ion for each pair of O atoms (one weakly, one strongly bound) is equal to the charge removed for each of the four I-O bonds in the periodates. The fraction of this charge due to the $5s$ electrons will be denoted by the hybridization parameter S^2 . We have the following relations:

$$Z_{\text{eff}} = 7.25 + 0.35m\Delta Z, \quad (14)$$

$$h_{5p} = m(1 - S^2)\Delta Z, \quad (15)$$

$$h_{5s} = mS^2\Delta Z, \quad (16)$$

where m is the number of I-O bonds. From Eq. (5) and the Fermi-Segrè formula, Eq. (3), we find to a first approximation

$$\Delta|\Psi_{5s}(0)|^2/|\Psi_0(0)|^2 = 0.097m\Delta Z. \quad (17)$$

However, hybridization reduces the number of $5s$ electrons to $2 - mS^2\Delta Z$ and Eq. (17) must be modified to

$$\Delta|\Psi_{5s}(0)|^2/|\Psi_0(0)|^2 = \frac{1}{2}(2 - mS^2\Delta Z)(1 + 0.097m\Delta Z) - 1. \quad (18)$$

Using our isomeric shift data for KIO_3 ($m=3$ ²⁵) and KIO_4 ($m=4$) we obtain two equations with unknowns ΔZ , $S^2(\text{KIO}_3)$, and $S^2(\text{KIO}_4)$. For the tetrahedral $(\text{IO}_4)^-$ configuration we take $S^2(\text{KIO}_4) = 0.25$ (see Ref. 19) and solve the equations for ΔZ and $S^2(\text{KIO}_3)$;

$$\Delta Z = 0.61, \quad (19)$$

$$S^2(\text{KIO}_3) = 0.02. \quad (20)$$

Equation (20) indicates that the hybridization in KIO_3 is small, as was to be expected. The iodine charge in $\text{KIO}_3 = 3\Delta Z - 1 = 0.83$ and that in $\text{KIO}_4 = 4\Delta Z - 1 = 1.44$. The value of $\Delta Z = 0.61$ for the I-O bond may be compared with the ionicity for this bond derived from electronegativity considerations: We get $I = 0.44$ from the work of Dailey and Townes²² and $I = 0.5$ from the work of Gordy.²⁰

IV. QUADRUPOLE COUPLING

The combination of a ZnTe source and an iodate absorber gives a spectrum (Fig. 6) that can be interpreted by pure quadrupole coupling in the iodate. Previous NMR measurements²⁶ on the I^{127} iodates have shown that the asymmetry parameter η is very small and can be neglected. Hence, it is possible to represent the positions of the hyperfine absorption lines by

$$\delta_{ij} = \frac{ceqQ_{\text{gnd}}}{4E_\gamma} \left[\frac{Q_{26.8}}{Q_{\text{gnd}}} C(I^*, m_j^*) - C(I, m_i) \right] + \delta', \quad (21)$$

where

$$C(I, m) = [3m^2 - I(I+1)]/I(2I-1),$$

δ_{ij} is the shift of the transition from the ground-state level $|I, m_i\rangle$ to the excited-state level $|I^*, m_j^*\rangle$, and δ'

²⁶ G. Ludwig, J. Chem. Phys. 25, 159 (1956).

is the isomeric shift of the iodate with respect to the ZnTe source. The states considered here have spins $I^* = \frac{5}{2}$ and $I = \frac{7}{2}$, and the transition between them has pure $M1$ character ($m_i - m_j = 0, \pm 1$) so that there are eight components. The $KI^{129}O_3$ ground-state coupling constant, $eqQ_{\text{gnd}} = 698.9$ Mc/sec, was calculated from the known $KI^{127}O_3$ coupling constant of 996.7 Mc/sec measured at 80°K ²⁷ and the accurately measured²⁸ quadrupole moment ratio, $Q_{129}/Q_{127} = +0.70121$. Figure 7 is a representation of Eq. (21) and demonstrates how the line positions change as a function of $Q_{26.8}/Q_{\text{gnd}}$. If we compare Fig. 7 with the measured spectrum of KIO_3 given in Fig. 6, we see that the observed structure is obtained for $Q_{26.8}/Q_{\text{gnd}} = +1.23$. The line intensities which for a thin polycrystalline absorber are proportional to the square of the Clebsch-Gordan coefficients ($|Im_i \Delta m| |Im_j^* m_j^*|$) are in agreement with the data.

The ratio $Q_{26.8}/Q_{\text{gnd}} = +1.23 \pm 0.02$ and the KIO_3 isomer shift $\delta' = 0.156 \pm 0.02$ cm/sec were deduced from the measured values of δ_{ij} for lines 2, 4, 6, 7, and 8 by least-squares fit to Eq. (21). This equation represents a straight line with slope $Q_{26.8}/Q_{\text{gnd}}$ and an intercept δ' . The value of $Q_{26.8}/Q_{\text{gnd}}$ derived from NH_4IO_3 was also $+1.23 \pm 0.02$. Because the iodate lines were not completely resolved, the errors assigned to δ' are larger than for the single line iodides. The KIO_3 and NH_4IO_3 quadrupole coupling constants, eqQ_{129} , which were determined from the spectra are in agreement with the more accurate NMR values²⁷ for the I^{127} iodates. From $Ba(IO_3)_2$ which has not been measured by NMR we obtained $eqQ_{127} = 1030 \pm 20$ Mc/sec at 80°K .

The sign of the field gradient q at the I^{129} nucleus

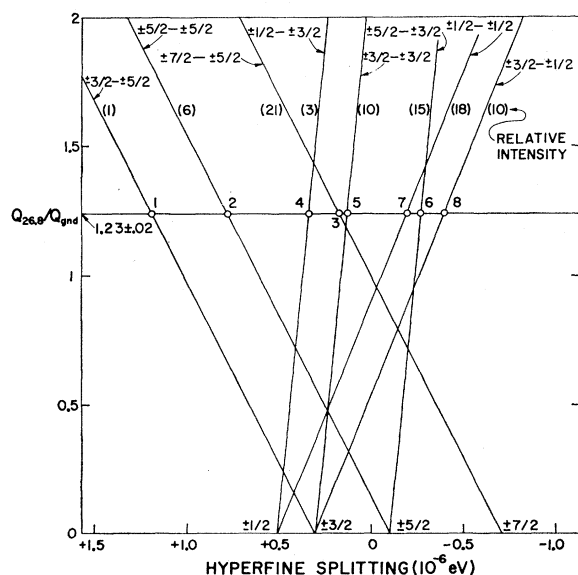


FIG. 7. KIO_3 line positions computed from Eq. (21) as a function of the quadrupole ratio $Q_{26.8}/Q_{\text{gnd}}$.

²⁷ F. Herlach, *Helv. Phys. Acta* **34**, 305 (1961).

²⁸ R. Livingston and H. Zeldes, *Phys. Rev.* **90**, 609 (1953).

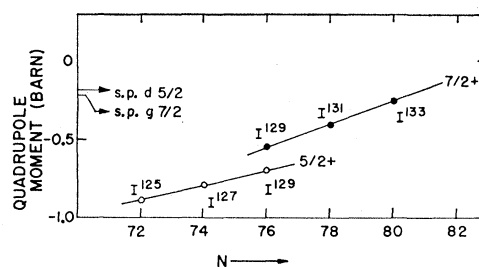


FIG. 8. Measured values of the iodine quadrupole moments for $I = \frac{5}{2}$ and $\frac{7}{2}$ versus the neutron number. The arrows represent the single particle estimates (Ref. 31).

follows directly from the asymmetry of the hyperfine pattern (see Figs. 6 and 7). This is true for nuclei in which at least one of the states has a spin larger than $\frac{3}{2}$. By considering, for instance, transitions number 2 ($\pm\frac{5}{2} \rightarrow \pm\frac{5}{2}$) and 6 ($\pm\frac{5}{2} \rightarrow \pm\frac{3}{2}$) both starting from the same ground state, we see in Fig. 6 that line 2 has higher energy than line 6. Thus the excited state with $m_j^* = \pm\frac{5}{2}$ lies higher than $m_j^* = \pm\frac{3}{2}$. This implies that eqQ is positive see [Eq. (21)]. Since the quadrupole moments of both the ground state and the 26.8-keV excited state are negative,²⁹ the sign of q is negative.

The values of $eqQ_{127} = 996.7$ Mc/sec for KIO_3 (80°K) and $eqQ_{127} = 2292.8$ Mc/sec for atomic iodine imply that there is about a 40% $5p$ -electron imbalance on the iodine in the iodate group. The field gradient caused by one p_z hole is $\frac{2}{5}e\langle 1/r^3 \rangle$ and is of the opposite sign when compared to the iodate q .

V. NUCLEAR RESULTS

1. The Iodine Quadrupole Moments

The six known iodine quadrupole moments are displayed in Fig. 8 as a function of their neutron number. Their systematic behavior has characteristics of both the collective model and the shell model. The data for Fig. 8 was obtained as follows: A value for the I^{127} quadrupole moment $Q_{127} = -0.79$ b has been measured²⁹ by atomic beam methods. By using this value and the experimentally determined Q ratios, $Q_{129}/Q_{127} = +0.70121$ measured by Livingston and Zeldes²⁸ and $Q_{26.8}/Q_{\text{gnd}} = +1.23 \pm 0.02$ for I^{129} (Sec. IV), we find for I^{129} : $Q_{\text{gnd}} = -0.55$ b and $Q_{26.8} = -0.68$ b. The values of Q for the other iodine isotopes were computed from the accurately determined Q/Q_{127} ratios listed in the Nuclear Data Sheets.²⁹

Figure 8 clearly shows that the value of $|Q|$ decreases linearly with the addition of pairs of neutrons. This decrease indicates that the polarization of the core is approximately proportional to the number of holes in the closed neutron shell $N = 82$. Calculations of Q in which the individual nucleons are coupled to the core

²⁹ *Nuclear Data Sheets*, compiled by K. Way *et al.* (Printing and Publishing Office, National Academy of Science—National Research Council, Washington 25, D. C.), NRC 61-1-130, Appendix I.

by a long-range quadrupole interaction have been carried out by Kisslinger and Sorensen³⁰ for these and other nuclei. Their results show a small decrease in $|Q|$ when approaching a closed neutron shell, but the decrease is not linear and their values of Q are not in quantitative agreement with the experimental values.

A linear extrapolation to the closed neutron shell $N=82$ (see Fig. 8) gives a value of $Q=-0.11$ b for the $\frac{7}{2}^+$ state in fair agreement with the single-particle estimate, whereas the extrapolated value of $|Q|$ for the $\frac{5}{2}^+$ state is much larger. This means that the three protons outside the $Z=50$ closed proton shell couple to give $|Q(\frac{7}{2})| < |Q(\frac{5}{2})|$. In contrast to the data, the calculations of Kisslinger and Sorensen,³⁰ the single-particle estimates,³¹ and the configuration mixing calculations of Horie and Arima³¹ all predict $|Q(\frac{7}{2})| > |Q(\frac{5}{2})|$.

2. The Change of Nuclear Radius $\Delta R/R$

From the calibration of the isomeric shift scale [Eq. (8), Sec. III.2] we can determine the I^{129} nuclear radius change, $\Delta R/R = (R_{26.8} - R_{\text{gnd}})/R_{\text{gnd}}$. To do this we must know $|\Psi_0(0)|^2$, the total $5s^2$ -electron density at the nucleus for the $5s^25p^6$ closed-shell configuration. This can be obtained from the Fermi-Dirac formula (3). Since the spectroscopic data for I^{6+} is incomplete, we have obtained the values of the effective quantum number $(n_a)^3 = 6.5$ and the quantum defect $(1 - d\sigma/dn) = 1.0975$ used in this formula by interpolation from data for other elements.¹⁰ Equation (10) gives the effective charge $Z_{\text{eff}} = 7.25$ for $h_p = 0$. From these data we find $|\Psi_0(0)|^2 = 2.0 \times 10^{27}/\text{cm}^3$.¹⁸ By combining this result with Eqs. (2) and (8) we obtain $\Delta R/R = 3 \times 10^{-5}$.

One might expect that the single-particle shell model would give a fair estimate of $\Delta R/R$ since the I^{129} nucleus has only three protons outside the closed shell $Z=50$, but our calculations of $\Delta R/R$ for this model are not in agreement with the data. Eisinger and Jaccarino³² have calculated the radial moments of protons in various single-particle states for a finite square-well potential. Using their results for a $g_{7/2}$ ground state and a $d_{5/2}$ excited state, we obtain $\Delta R/R = -2 \times 10^{-3}$ which disagrees in sign and is a factor of 100 greater than the experimental value. If we take into account various configurations of the three protons, we can obtain the proper sign of $\Delta R/R$ but not the magnitude. For instance, the ground-state configuration $[g_{7/2}(d_{5/2})^2]_{7/2}$ and the excited-state configuration $[d_{5/2}(g_{7/2})^2]_{5/2}$ gives $\Delta R/R = 3 \times 10^{-3}$. Because of these results and those of Horie and Arima (Sec. V.1) it appears that a more complete configuration-mixing calculation is necessary but perhaps not sufficient to reconcile the shell model with our experimental results. These estimates of $\Delta R/R$ are,

of course, dependent on the shape that has been assumed for the nuclear potential. For example, the spherical harmonic oscillator which is less suitable for the nuclear potential than the finite square well gives $\langle r^2_{10} \rangle = \langle r^2_{20} \rangle$. This implies that a nuclear harmonic oscillator would have $\Delta R/R = 0$ for the configurations discussed above.

On the other hand, by using the method of Barrett and Shirley,³³ we can also semiquantitatively calculate $\Delta R/R$ by considering the collective nuclear deformation ϵ derived from the quadrupole moments. Since the collective contribution to the I^{129} quadrupole moment is much larger than that due to the single particle (Sec. V.1), we can relate the spectroscopic quadrupole moment Q to the intrinsic quadrupole moment Q_0 and the deformation parameter ϵ by

$$Q \cong P(x)Q_0 = P(x) \frac{2}{5} Z \epsilon R_0^2 (1 + \epsilon/2 + \dots), \quad (22)$$

where $P(x)$ is the projection factor discussed by Bohr and Mottelson³⁴ and R_0 is the mean nuclear radius. $P(x) = 1$ in the limit of weak coupling between core and particle, and $P(x) = I(2I-1)/(I+1)(2I+3)$ for strong coupling. If the deformed nucleus is assumed to be an incompressible, uniformly charged ellipsoid bound by the surface $R = R_0(1 + (2\epsilon/3)P_2(\cos\theta))$, we find:

$$\Delta R/R = \frac{1}{2} (R_{\text{ex}}^2 - R_{\text{gnd}}^2) / R_{\text{gnd}}^2 = (2/9) \Delta(\epsilon^2). \quad (23)$$

Since Q is known for both states of I^{129} (Sec. V.1), we can compute the two values of ϵ from Eq. (22) and then $\Delta R/R$ from Eq. (23). The results are $\Delta R/R = 1 \times 10^{-4}$ for the weak-coupling limit and $\Delta R/R = 2 \times 10^{-3}$ for the strong-coupling limit. Both values agree in sign with the experimental value. The fair agreement between the experimental value of $\Delta R/R$ and the weak coupling result is confirmed by the values of Bohr and Mottelson for $P(x)$ in neighboring nuclei (In and Sb).

3. Lifetime of the 26.8-keV State in I^{129}

The absorption linewidth is broadened by the thickness of the absorber [see Eq. (24)]. Extrapolating the line width obtained with LiI, NaI, and CsI to zero thickness (see Fig. 9), we find a width Γ corresponding to a lifetime $\tau = 2\hbar/\Gamma = 20$ nsec for the 26.8-keV state. This value should be considered as a lower limit because of the possibility of solid state broadening. It is smaller than the two electronic measurements of 26.8 ± 1.5 nsec,³⁵ 23 ± 1.9 nsec,³⁶ and 20.3 ± 1.5 nsec³⁷ recently reported.

By combining the internal conversion coefficient

³⁰ L. S. Kisslinger and R. A. Sorensen, Rev. Mod. Phys. **35**, 853 (1963).

³¹ H. Horie and A. Arima, Phys. Rev. **99**, 778 (1955).

³² J. Eisinger and V. J. Jaccarino, Rev. Mod. Phys. **30**, 528 (1958).

³³ P. Barrett and D. Shirley, Phys. Rev. **131**, 123 (1963).

³⁴ A. Bohr and B. Mottelson, Kgl. Danske Videnskab. Selskab, Mat. Fys. Medd. **27**, No. 16 (1953).

³⁵ H. deWaard, M. Garrell, and D. Hafemeister, Phys. Letters **3**, 59 (1962).

³⁶ I. M. Govil, C. S. Khurana, and H. S. Hans, Nucl. Phys. **45**, 60 (1963).

³⁷ S. Jha and R. Leonard (to be published).

$\alpha = 5.4^{38,39}$ with our value of τ , we obtain the γ lifetime, $\tau_\gamma = 160$ nsec. The value of τ_γ corresponds to a retardation factor of 140 with respect to the single particle $M1$ estimate.

4. Magnetic Splitting in $\text{Cr}_x\text{Te}_y^{129}$

A ferromagnetic $\text{Cr}_x\text{Te}_y^{129}$ source and KIO_4 absorber gave an unresolved pattern broadened by a factor of 7. The magnetic field at the iodine nucleus inferred from the line broadening is approximately 70 kG. This may be compared with the results (50 kG at the Te nucleus) of a recent Mössbauer experiment⁴⁰ on $\text{Cr}_x\text{Te}_y^{125}$. Since the 18 hyperfine lines were not resolved in the Cr_xTe_y spectrum, we can only conclude that the magnetic moment of the 26.8-keV state is not too different from that of the ground state. Recently, the magnetic moment of the 26.8-keV state has been determined more accurately by Heberle and deWaard.⁴¹ They have used the 50-kG field of a superconducting magnet to produce a Zeeman effect in a KI^{129} absorber. They report a value $\mu_{26.8}/\mu_{\text{gnd}} = 1.07 \pm 0.07$.

VI. RECOILLESS FRACTIONS IN THE ALKALI IODIDES

The recoilless fraction f' of the alkali iodides at 80°K has been determined from the dependence on the absorber thickness of the width and the area of the absorber line. Since all alkali iodides have a cubic crystal structure, all give a single line absorption in combination with a ZnTe source (Fig. 3).

1. Linewidth Method

For the range of absorber thicknesses used in this experiment, the experimental absorption linewidth Γ_{exp} increases (Fig. 9) linearly with thickness t and has been given by O'Connor⁴² as

$$\Gamma_{\text{exp}} = \Gamma_a + \Gamma_s + 0.27\Gamma_{\text{nat}}n\sigma_0 t f', \quad (24)$$

where Γ_a , Γ_s , and Γ_{nat} are the absorber, source and natural linewidths, nt is the number of atoms/cm² capable of resonant absorption, and f' is the absorber recoilless fraction. σ_0 is the absorption cross section at resonance given by

$$\sigma_0 = 2\pi\lambda^2 \frac{2I^* + 1}{2I + 1} \frac{1}{1 + \alpha_T} \frac{\Gamma_{\text{nat}}}{\Gamma_a}, \quad (25)$$

where $2\pi\lambda$ is the wavelength of the γ ray, I^* and I are the nuclear spins of the excited and ground states,

³⁸ M. E. Rose, *Internal Conversion Coefficients* (North-Holland Publishing Company, Amsterdam, 1958).

³⁹ L. A. Sliv and I. M. Band, Leningrad Physico-Technical Institute Reports, 1956 and 1958 (unpublished) [translation: Reports 57ICC K1 and 57ICC L1, issued by Physics Department, University of Illinois, Urbana, Illinois (unpublished)].

⁴⁰ N. Shikazono, *J. Phys. Soc. Japan* **18**, 925 (1963).

⁴¹ J. Heberle and H. deWaard, *Bull. Am. Phys. Soc.* **9**, 452 (1964).

⁴² D. A. O'Connor, *Nucl. Instr. Methods* **21**, 318 (1963).

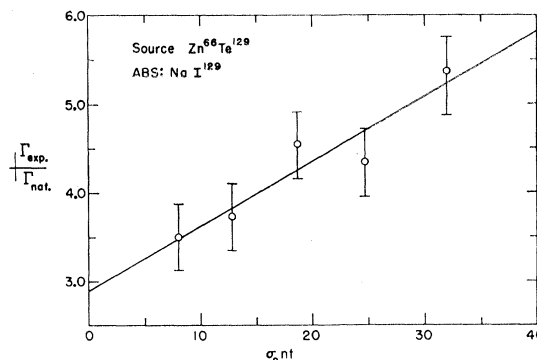


FIG. 9. Experimental linewidth relative to natural width versus I^{129} effective thickness ($n\sigma_0 t$) for NaI.

respectively, and α_T is the total internal conversion coefficient for the transition. We have determined the value of nt from the activity (Sec. II.3), $\alpha_T = \alpha_{L+M} = 5.4$ from the average of the values^{42a} computed by Rose,³⁸ and Sliv and Band,³⁹ and $\Gamma_{\text{nat}} = 0.030$ cm/sec from the average of two electronic lifetime measurements (Sec. V.3). The relative linewidth, $\Gamma_{\text{exp}}/\Gamma_{\text{nat}}$, has been plotted for LiI, NaI, and CsI as a function of $n\sigma_0 t$ (e.g., Fig. 9). The determination of the slopes of these plots by a least-squares fit to the data yields f' directly. The results are given in Table III and Fig. 12. The large Rb photoelectric cross section lowered the signal to background ratio so as to make the Rb data unacceptable for this method of analysis.

2. Area Method

The absorption line areas are of particular interest because they are independent of source line shape and instrumental velocity resolution and because they

TABLE III. The ratio of recoilless fraction, f'/f'_{NaI} , determined by the area method, the fraction f' determined by the linewidth method; the nearest-neighbor central force constant, $C_{11} \times a_0$; the lattice spacing a_0 ; and the Debye temperature for the alkali iodides at 80°K.

Alkali iodide	f'/f'_{NaI} Area method	f' Linewidth method	$C_{11} \times a_0$ force constant	θ_D
LiI	1.0 ± 0.3	0.23 ± 0.05	8.6×10^8	311°K ^a
NaI	1	0.29 ± 0.05	9.8×10^8	185°K ^b
KI			9.8×10^8	157.5°K ^b
RbI	0.8 ± 0.2		9.5×10^8	120°K ^c
CsI	0.9 ± 0.2	0.24 ± 0.05		96°K ^d

^a A. Karo, *J. Chem. Phys.* **31**, 1498 (1959).

^b W. Berg and J. A. Morrison, *Proc. Roy. Soc. (London)* **A242**, 467 (1957).

^c K. Clusius, J. Goldman, and A. Perlick, *Z. Naturforsch.* **4**, 424 (1949).

^d G. Jones, D. Martin, P. Mawer, and C. Perry, *Proc. Roy. Soc. (London)* **A261**, 10 (1961).

^{42a} The internal conversion coefficient of the 26.8-keV state of I^{129} has recently been measured by S. H. Devare and H. G. Devare, *Phys. Rev.* **134**, B705 (1964). Their value of 4.5 ± 0.5 is in good agreement with the calculated values.

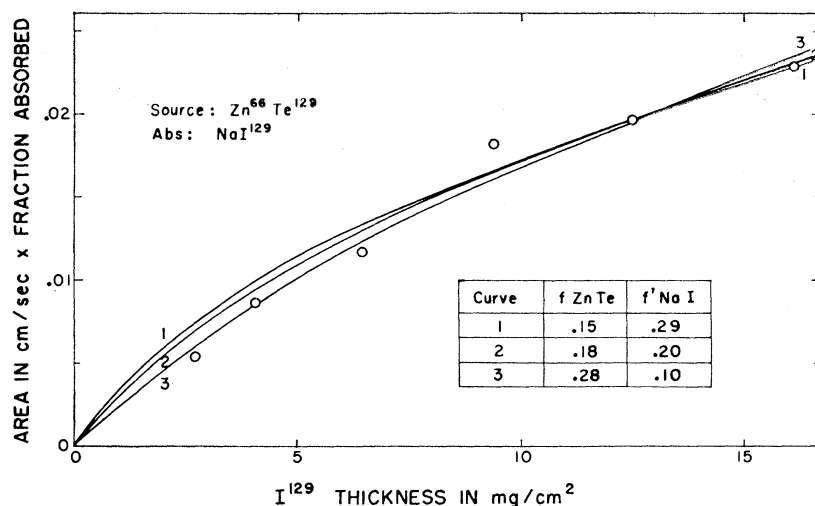


FIG. 10. Resonance absorption area versus I^{129} thickness for NaI. The curves have been computed from the f and f' values in the table.

saturate less rapidly with increasing absorber thickness than the associated absorption amplitudes. In order to correct for the background, we have multiplied the areas by the ratio $(N_{26.8} + N_{\text{bkg}})/N_{26.8}$, where $N_{26.8}$ and N_{bkg} are the total number of 26.8-keV and background counts observed in a particular experimental run. This factor ranged from 1.2 for the thinnest LiI absorber to 2.7 for the thickest RbI absorber.

Lang⁴³ has recently computed the absorption area as a function of the source recoilless fraction f and the effective thickness $T = n\sigma_0 t$. We have applied his calculations with the f and f' values given in the table in Fig. 10 to compute the curves shown there. We observe from Fig. 10 that this method is relatively insensitive for the simultaneous determination of both f and f' . Because of this we have determined the ratio f'/f'_{NaI} from the area method rather than f and f' directly. We have adopted the values $f'_{\text{NaI}} = 0.29$ obtained in Sec. VI.1 and $f_{\text{ZnTe}} = 0.15$ (curve 1, Fig. 10) to compute the curves of Fig. 11. These curves indicate

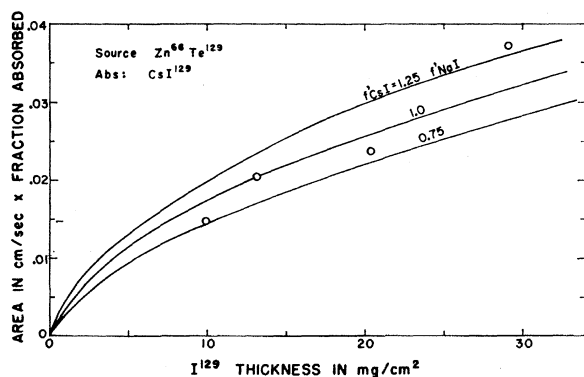


FIG. 11. Resonance absorption area versus I^{129} thickness for CsI. The curves have been computed on the basis of the f and f' values of curve 1 of Fig. 10.

⁴³ G. Lang, Nucl. Instr. Methods 24, 425 (1963).

that f'_{CsI} is approximately equal to f'_{NaI} . The possibility of an inhomogeneous distribution of alkali iodide powder and the uncertainty in the large background corrections (especially for RbI and CsI) are the causes for the large errors indicated in Table III.

3. Comparison with Theory

Both methods just described (see Table III) indicate that f' varies by less than 25% over the alkali iodides. These data are compared with the available theoretical predictions in Fig. 12 and in the following discussion.

The recoilless fraction f has been calculated¹ for monatomic lattices using the Debye approximation and the result is called the Debye-Waller factor. When the specific-heat Debye temperatures of the alkali iodides (Table III) are inserted in the Debye-Waller factor, a large variation of f' follows (from 0.79 in LiI to 0.15 in CsI at 80°K). It is not surprising that these calculations intended for monatomic lattices do not agree with our diatomic data. However, it is interesting to note the fair agreement between the experimental value of f' for CsI and the value computed from the Debye temperatures (Fig. 12). One would expect the Debye approximation to be most successful when the mass difference between alkali and halogen atoms is small.

Kagan and Maslov³ have calculated f for the diatomic NaCl lattice. Their results are given in terms of the C_{11} and C_{44} elastic constants and the atomic masses. We have used the accurately determined elastic constants of Spangenberg and Haussühe⁴⁴ with their results to compute the alkali iodide f' s. These values are lower in magnitude and more dependent on the mass ratio than our data (see Fig. 12).

Hofmann *et al.*⁴⁵ have fitted their specific-heat data

⁴⁴ K. Spangenberg and S. Haussühe, Z. Krist. 109, 422 (1957).

⁴⁵ J. Hofmann, A. Paskin, K. Tauer, and R. Weiss, Phys. Chem. Solids 1, 45 (1956).

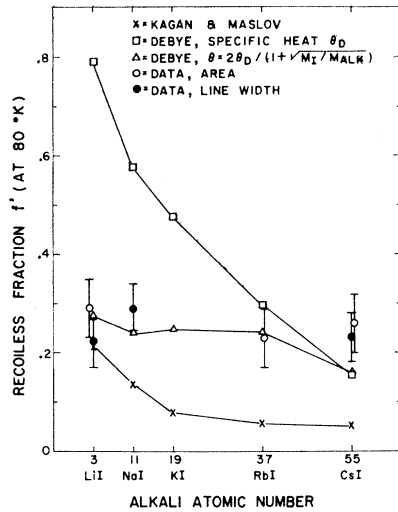


FIG. 12. Theoretical and experimental values of f' for the alkali iodides at 80°K. The data for the area method were computed on the basis of $f'_{\text{NaI}} = 0.29$.

for diatomic compounds by considering the Debye temperature θ_D to be

$$\theta_D = \frac{1}{2}(\theta_A + \theta_B). \quad (26)$$

θ_A and θ_B , the Debye temperatures for the elements A and B in the diatomic compound, may be related by their masses for $T > \theta_D$ by

$$\theta_A/\theta_B = (m_B/m_A)^{1/2}. \quad (27)$$

Combining these equations, we obtain an effective Debye temperature for iodine in a diatomic lattice

$$\theta_I = 2\theta_D / [1 + (m_I/m_{\text{alk}})^{1/2}]. \quad (28)$$

Inserting θ_I in the Debye-Waller factor, we obtain an f' which is approximately a constant for the alkali iodides as is shown in Fig. 12.

One explanation for the small variation of f is as follows: The nearest-neighbor central atomic-force constant, $C_{11} \times a_0$ (a_0 is the lattice spacing) varies by only 10% for the various alkali iodides (Table III). This implies that the iodine ion must be situated in a similar potential well in all of the alkali iodides and therefore should exhibit a reasonably constant recoilless fraction. This interpretation is analogous to the results of Maradudin and Flinn⁴⁶ who have calculated f for an impurity atom. They have shown that at higher temperatures (80°K for our case) f will be approximately a constant for a fixed spring constant and will be only slightly dependent on the mass ratio.⁴⁷

ACKNOWLEDGMENTS

We thank P. Axel, P. Debrunner, W. Flygare, H. Frauenfelder, G. Goodman, R. Ingalls, G. Kane, H. Lipkin, D. Pipkorn, and C. P. Slichter for many interesting and useful discussions. We are grateful to G. Beck and P. Hesselman for the many reactor irradiations.

⁴⁶ A. Maradudin and P. Flinn, Phys. Rev. **126**, 2059 (1962).

⁴⁷ Recently Fitch et al. [D. Fitch, R. Silsbee, T. Fulton, and E. Wolf, Phys. Rev. Letters **11**, 275 (1963)] have observed zero phonon transitions of color centers in the alkali halides using optical absorption techniques. They have measured the temperature dependence of the intensity of the zero phonon line and from this they have determined the characteristic temperatures for the process. In contrast to our Mössbauer results, they have found characteristic temperatures not too different from the alkali halide Debye temperatures.